

IMECE2008-66227

## COUPLED THERMOELASTIC VIBRATIONS ANALYSIS OF FUNCTIONALLY GRADED TIMOSHENKO BEAMS USING THE GALERKIN FINITE ELEMENT METHOD

**M. ABBASI**

Mechanical Engineering Dept.,  
Amirkabir University of Technology,  
Tehran, Iran  
Musan.abbasi@gmail.com

**M. SABBAGHIAN**

Mechanical Engineering Dept.,  
Louisiana State University,  
Baton Rouge, Louisiana, USA  
mehdys@bellsouth.net

**M. R. ESLAMI**

Mechanical Engineering Dept.,  
Amirkabir University of Technology,  
Tehran, Iran  
eslami@aut.ac.ir

### ABSTRACT

This paper presents the finite element solution of a Timoshenko beam with functionally graded material (FGM) subjected to lateral thermal shock loads. The FGM beam is assumed to be graded across the thickness. The material properties across the thickness direction follow the volume fraction of the constitutive materials in power law form. The solution is obtained under coupled thermoelastic assumption. The equation of motion and the conventional coupled energy equation are simultaneously solved to obtain the transverse deflection and temperature distribution in the beam. The governing partial differential equations of the problem are solved simultaneously using the Galerkin finite element method with the  $C^1$ -continuous shape function leading to fast convergence of the solution. Results are presented for different power law indexes and coupling coefficients for simply supported boundary conditions. The results are verified with those reported in the literature.

### INTRODUCTION

The equations for a coupled thermoelastic beam, including the effects of shear deformation and rotatory inertia, are derived by Jones [1]. McQuillen and Brull [2] presented an analytical solution for the dynamic thermoelastic response of cylindrical shells using the variational theorem. Coupled thermally induced vibrations of Euler-Bernoulli and Timoshenko beams with one dimensional heat conduction are investigated by Seibert and Rice [3]. Coupled thermoelasticity

of beams made of homogeneous and isotropic material is discussed by Massalas and Kalpakidis [4,5]. The analytical solution of the coupled thermoelasticity of beams with the Euler-Bernoulli assumption is given in reference [4], and that with Timoshenko assumption is given in reference [5]. In the treatment of these problems a linear approximation for temperature variation across the thickness direction of the beam is considered. Eslami and Vahedi presented the one-dimensional coupled thermoelasticity problem of rods with classical coupled assumption using the Galerkin finite element method [6].

Finite element coupled thermoelastic analysis of composite Timoshenko-beams is given by Maruthi and Sinha [7], where the temperature variation across the thickness direction is neglected. Coupled thermoelastic behavior of shells of revolution is analyzed by Eslami et al [8]. Manoach and Ribeiro developed a numerical procedure to study the coupled large amplitude thermoelastic vibrations of Timoshenko beams subjected to the thermal and mechanical loads using the finite difference approximation and modal coordinate transformations [9]. Sankar solved the elastic problem of FGM beam and computed the thermal stresses in an FGM Euler-beam based on the uncoupled thermoelasticity assumption [10, 11].

This paper presents the vibration behavior of an FGM Timoshenko beam under lateral thermal shock with coupled thermoelastic assumption. The analysis is based on the Galerkin finite element method, using a  $C^1$ -continuous shape function.

## DERIVATION OF THE GOVERNING EQUATIONS

Consider a beam of rectangular cross section with length  $l$ , height  $h$ , and width  $b$ , as shown in fig. 1. Using the Timoshenko beam theory, the displacement components are

$$\begin{aligned} u(x, z, t) &= u_0(x, t) - z\psi(x, t) \\ w(x, t) &= w(x, t) \end{aligned} \quad (1)$$

where  $u$  is the axial displacement component,  $u_0$  is the displacement of a point on the reference plane,  $w$  is the lateral deflection,  $\psi$  is the rotation angle of the cross-section with respect to the longitudinal axis,  $z$  is measured across the thickness direction from the middle plane of the beam at  $x=0$  and  $t$  stands for time variable, respectively. A comma in subscript indicates partial differentiation.

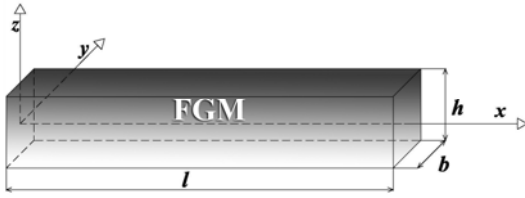


**Fig. 1:** The beam and coordinates

The FGM profile across the thickness direction of the beam, made of ceramic and metal constituent materials, may be assumed to follow a power law form as

$$f(z) = f_m + f_{cm} \left( \frac{2z+h}{2h} \right)^n \quad (2)$$

where  $f$  is any material property of the FGM,  $f_m$  is metal property of FGM,  $f_{cm} = f_c - f_m$ ,  $f_c$  being the ceramic property of FGM, and  $n$  is the power law index, respectively. The density, modulus of elasticity, coefficient of specific heat, coefficient of thermal expansion, and the conduction coefficient may be assumed to follow the power law form, indicated by eq. (2).

The location of the neutral axis of an FGM beam graded across the thickness is obtained as

$$z_{NA} = \frac{\int_z \rho(z)z dz}{\int_z \rho(z) dz} \quad (3)$$

where  $NA$  is a symbol for the neutral axis and the integration is across the cross sectional area of the beam. For this formulation,  $z$ -coordinate is measured across the thickness direction from the FGM beam neutral axis.

Assuming that the beam material is linear elastic, the stress-strain relations for the FGM beam based on the assumed displacement components, including the shear deformation, are [9]

$$\begin{aligned} \sigma_x &= E(z)[\varepsilon_x - \alpha(z)\theta] \\ \sigma_{xz} &= k_s G(z)\varepsilon_{xz} \end{aligned} \quad (4)$$

where  $E$  is the modulus of elasticity,  $G$  is the shear modulus,  $k_s$  is the shear correction factor,  $\alpha$  is the coefficient of thermal expansion,  $\theta = T - T_0$  is the temperature change, and  $T_0$  is the reference temperature, respectively.

The bending moments, the shear force, and the in-plane stress resultants per unit length are expressed by the stresses as follows:

$$\begin{aligned} N &= \int_z \sigma_x dz \\ M &= \int_z \sigma_x z dz \\ Q &= \int_z \sigma_{xz} dz \end{aligned} \quad (5)$$

The temperature change across the thickness direction is assumed to be linear. This assumption is justified considering that the thickness of the beam is small with respect to its length [4, 5] thus

$$\theta = \theta_1(x, t) + \frac{z}{h} \theta_2(x, t) \quad (6)$$

where  $\theta_1$  and  $\theta_2$  are unknowns to be found across the beam's height and are coupled with displacement components of the beam.

### Equation of motion

The equations of motion of a beam based on Timoshenko theory is [9]:

$$\begin{aligned} N_{,x} &= I_0 u_{0,tt} - I_1 \psi_{,tt} \\ M_{,x} - Q &= I_1 u_{0,tt} - I_2 \psi_{,tt} \\ Q_{,x} &= I_0 w_{,tt} - p(x, t) \end{aligned} \quad (7)$$

where  $p$  is the applied surface lateral mechanical loading which is zero in this analysis,  $I_i = \int_z \rho(z)z^i dz$  ( $i=0,1,2$ ) are the mass moment of inertia and  $\rho$  is the mass density of the beam, respectively.

Substituting eqs. (4), (5) and (6) into eq. (7), and neglecting  $u_0$  and the axial inertia effects the equations of motion become

$$\begin{aligned} A_1 \psi_{,xx} + A_2 \psi + A_3 w_{,x} + A_4 \theta_{1,x} + A_5 \theta_{2,x} + A_6 \psi_{,tt} &= 0 \\ B_1 \psi_{,x} + B_2 w_{,xx} + B_3 w_{,tt} &= 0 \end{aligned} \quad (8)$$

where the  $A$ 's and  $B$ 's are the constants of eq. (8). Simply supported boundary conditions are considered for the beam and the beam is assumed to be initially at zero deflection

$$\begin{aligned}
\psi_{,x}(0,t) = \psi_{,x}(l,t) = 0, & \quad t > 0 \\
w(0,t) = w(l,t) = 0, & \quad t > 0 \\
\psi(x,0) = w(x,0) = 0. & \quad 0 \leq x \leq l
\end{aligned} \quad (9)$$

### Energy equations

The first law of thermodynamics for heat conduction in beam in the coupled form is [6]

$$(k\theta_{,i})_{,i} - \rho c_v \theta_{,t} - \alpha T_0 (3\lambda + 2\mu) (\varepsilon_{ii})_{,t} = 0 \quad (10)$$

where  $k$ ,  $c_v$ , and  $\varepsilon_{ii}$  are the thermal conductivity, specific heat, and normal strain, respectively, and  $\lambda$  and  $\mu$  are the Lamé constants. The energy equation for the beam based on Timoshenko theory is reduced to

$$Res = k\theta_{,xx} + k\theta_{,zz} - \rho c_v \theta_{,t} + E\alpha T_0 z \psi_{,xt} = 0 \quad (11)$$

The thermal boundary conditions may be assumed in form of an applied heat flux  $q$ , convection  $h_c$ , or specified temperature shock on the upper or lower surfaces of the beam. The energy equation is obtained assuming that the upper surface of the beam is exposed to a heat flux  $q(x,t)$  and the lower surface is under convection to the ambient with the coefficient  $h_c$ .

The beam is initially assumed to be at ambient temperature and the thermal boundary and initial conditions are assumed as

$$\begin{aligned}
\theta(0,t) = \theta(l,t) = 0, & \quad t > 0 \\
\theta(x,0) = 0. & \quad 0 \leq x \leq l
\end{aligned} \quad (12)$$

Using eq. (6) and multiplying eq. (11) by  $dz$  and  $zdz$ , integrating over height  $h$ , the residue  $Res$  of the energy equation may be made orthogonal with respect to  $dz$  and  $zdz$ , to provide two independent equations for two independent functions  $\theta_1$  and  $\theta_2$  as

$$\begin{aligned}
C_1\theta_{1,xx} + C_2\theta_{2,xx} + C_3\theta_{1,t} + C_4\theta_{2,t} + C_5\psi_{,xt} + C_6\theta_2 \\
+ C_7q(x,t) = 0 \\
D_1\theta_{1,xx} + D_2\theta_{2,xx} + D_3\theta_2 + D_4\theta_{1,t} + D_5\theta_{2,t} + D_6\psi_{,xt} + \\
D_7\theta_2 + D_8q(x,t) = 0
\end{aligned} \quad (13)$$

where  $D$ 's and  $E$ 's are the constants of eq. (13).

### SOLUTION PROCEDURE

To solve the simultaneous governing equations, dimensionless values are defined as

$$\bar{w} = \lambda_1 \frac{K_c}{q_{ave} \alpha_c L} \psi$$

$$\begin{aligned}
\bar{w} &= \lambda_2 \frac{K_c}{q_{ave} \alpha_c L^2} w \\
\bar{x} &= \lambda_3 \frac{x}{L} \\
\bar{t} &= \lambda_4 \frac{\kappa_c}{h^2} t \quad \kappa_c = \frac{K_c}{\rho_c c_c} \\
\bar{\theta} &= \lambda_5 \frac{\theta}{T_0}
\end{aligned} \quad (14)$$

where  $q_{ave}$  and  $\kappa_c$  are the average heat flux at the top of the beam and thermal diffusivity, respectively. The bar values indicate dimensionless parameters. The parameters  $\lambda_i$  are dimensionless parameters introduced to enable the balance of the members of matrices in the FEM part of the solution. By changing  $\lambda_i$  more balance FEM matrices including stiffness, capacitance, and mass matrices are obtained leading to convergence of the solution.

Using the dimensionless parameters, the four coupled governing equations are

$$\begin{aligned}
a_1 \bar{w}_{,xx} + a_2 \bar{w} + a_3 \bar{w}_{,x} + a_4 \bar{\theta}_{1,x} + a_5 \bar{\theta}_{2,x} + a_6 \bar{w}_{,tt} = 0 \\
b_1 \bar{w}_{,x} + b_2 \bar{w}_{,xx} + b_3 \bar{w}_{,tt} = 0 \\
c_1 \bar{\theta}_{1,xx} + c_2 \bar{\theta}_{2,xx} + c_3 \bar{\theta}_{1,t} + c_4 \bar{\theta}_{2,t} + c_5 \bar{w}_{,xt} + c_6 \bar{\theta}_2 + c_7 q = 0 \\
d_1 \bar{\theta}_{1,xx} + d_2 \bar{\theta}_{2,xx} + d_3 \bar{\theta}_2 + d_4 \bar{\theta}_{1,t} + d_5 \bar{\theta}_{2,t} + d_6 \bar{w}_{,xt} + d_7 \bar{\theta}_2 \\
+ d_8 q = 0
\end{aligned} \quad (15)$$

where  $a$ 's,  $b$ 's,  $c$ 's and  $d$ 's are dimensionless constants of coupled equations. Simultaneous solution of these equations provides the distribution of the displacement components of the beam and the temperature variables.

### Laplace transform

The system of coupled equations (15) are functions of the space variable  $x$  and time  $t$ . Traditional finite element solution for such problems is the time marching method. The solution presented in this paper is obtained by transfinite element method, where time is eliminated using the Laplace transform. Once the finite element solution in space domain is obtained, a numerical scheme is used for the inverse Laplace transform to find the final solution in real time domain. Applying the Laplace transform to eqs. (15), gives

$$\begin{aligned}
a_2 \bar{\Psi}_{,xx} + a_3 \bar{\Psi} + a_4 \bar{W}_{,x} + a_4 \bar{\Theta}_{1,x} + a_5 \bar{\Theta}_{2,x} + s^2 a_6 \bar{\Psi} = 0 \\
b_1 \bar{\Psi}_{,x} + b_2 \bar{W}_{,xx} + s^2 b_3 \bar{W} = 0 \\
c_1 \bar{\Theta}_{1,xx} + c_2 \bar{\Theta}_{2,xx} + s c_3 \bar{\Theta}_1 + s c_4 \bar{\Theta}_2 + s c_5 \bar{\Psi}_{,x} + c_6 \bar{\Theta}_2 \\
+ c_7 Q = 0 \\
d_1 \bar{\Theta}_{1,xx} + d_2 \bar{\Theta}_{2,xx} + d_3 \bar{\Theta}_2 + s d_4 \bar{\Theta}_1 + s d_5 \bar{\Theta}_2 + s d_6 \bar{\Psi}_{,x} \\
+ d_7 \bar{\Theta}_2 + d_8 Q = 0
\end{aligned} \quad (16)$$

where  $s$  is the Laplace transform parameter and

$$\begin{aligned}\Psi &= L[\bar{\psi}], \\ W &= L[\bar{w}], \\ \Theta_1 &= L[\bar{\theta}_1], \\ \Theta_2 &= L[\bar{\theta}_2].\end{aligned}\quad (17)$$

#### Finite element modeling

The coupled system of eqs. (16) may be solved by the Galerkin finite element method. The beam is divided into a number of straight elements. The base element  $e$  along the length of the beam is considered. The unknown functions may be approximated with a third order interpolation function  $N$  as

$$\begin{aligned}\bar{\Psi} &= \langle \Psi_p \rangle \{N_p\} \\ \bar{W} &= \langle W_p \rangle \{N_p\} \\ \bar{\Theta}_1 &= \langle \Theta_{1,p} \rangle \{N_p\} \\ \bar{\Theta}_2 &= \langle \Theta_{2,p} \rangle \{N_p\} \quad p=1,2,3,4\end{aligned}\quad (18)$$

Considering a  $C^1$ -continuous shape function, the degrees of freedom for the element lateral deflection, for instance  $W_p$  becomes

$$\langle W_p \rangle = \langle \bar{W}_i \quad \bar{W}_{,\bar{x}}|_i \quad \bar{W}_j \quad \bar{W}_{,\bar{x}}|_j \rangle \quad (19)$$

where  $\bar{W}_{,\bar{x}}|_i$  and  $\bar{W}_{,\bar{x}}|_j$  are the  $x$ -derivatives of  $W$  at nodes  $i$  and  $j$ . Similar approximation is considered for  $\Theta_1$  and  $\Theta_2$ . The third order  $C^1$ -continuous shape functions  $N$  are

$$\begin{aligned}N_1 &= 1 - 3\left(\frac{\bar{x}}{\bar{l}}\right)^2 + 2\left(\frac{\bar{x}}{\bar{l}}\right)^3 \\ N_2 &= \bar{x}\left(1 - \frac{\bar{x}}{\bar{l}}\right)^2 \\ N_3 &= 3\left(\frac{\bar{x}}{\bar{l}}\right)^2 - 2\left(\frac{\bar{x}}{\bar{l}}\right)^3 \\ N_4 &= (\bar{x} - \bar{l})\left(\frac{\bar{x}}{\bar{l}}\right)^2\end{aligned}\quad (20)$$

where  $\bar{l}$  is the length of the base element.

The assumed shape functions insure the continuity of the nodal degrees of freedom as well as their first derivative with respect to the variable  $x$ . Now, the formal Galerkin method may be applied to the system of eqs. (16). This is done by making the residue of each of eqs. (16) for the base element orthogonal with respect to the approximating functions (20). The final finite element equation of motion, after assembling the matrix equations of each individual element, is obtained as

$$([M]s^2 + [C]s + [K])\{X\} = \{F\} \quad (21)$$

where  $[M]$ ,  $[C]$ ,  $[K]$ , and  $\{F\}$  are mass, capacitance, stiffness, and force matrices, respectively. Matrix  $\{X\}$  is the matrix of unknowns containing eight unknowns. The solution of eq. (21) for the unknown matrix  $\{X\}$  is obtained in terms of the Laplace parameter  $s$ . To obtain the solution in real time domain, the inverse Laplace transform must be carried out. This may be done numerically by the method proposed by Durbin [13].

## RESULTS

To validate the formulations, the results of this paper are compared with the analytical solution of a homogeneous beam reported in reference [4]. An aluminum beam of length 0.25m and height 0.0022m with simply supported boundary conditions is assumed. The ends of the beam are assumed to be at ambient temperature  $T_0 = 293^\circ\text{K}$ . The upper surface of the beam is exposed to a step function heat flux of intensity  $q = 10^8 \text{ W/m}^2$ , while the lower surface is assumed to be thermally insulated. Figure 2 shows the midpoint lateral deflection history of the heated beam for the coupled thermoelasticity assumptions reported by reference [4] and the present study. Figure 3 shows temperature change history between upper and lower surfaces at the midpoint of the heated beam for the coupled thermoelasticity assumptions reported by reference [4] and the present study. It is seen that the temperature history obtained by the coupled solution is diffused along the time and oscillated about a constant value with very small variations. Close agreements are observed between the two studies.

Consider an FGM beam with ceramic upper surface and metal lower surface. The material properties of metal and ceramic are given in Tab.1. The mechanical boundary conditions at the ends of the beam are assumed to be simply supported. The thermal boundary conditions at the ends of the beam are assumed to be at ambient temperature at  $T_0 = 293^\circ\text{K}$ . The total length of the beam is taken to be 0.8m and the thickness of the beam is 0.0025m. The upper side of the beam is

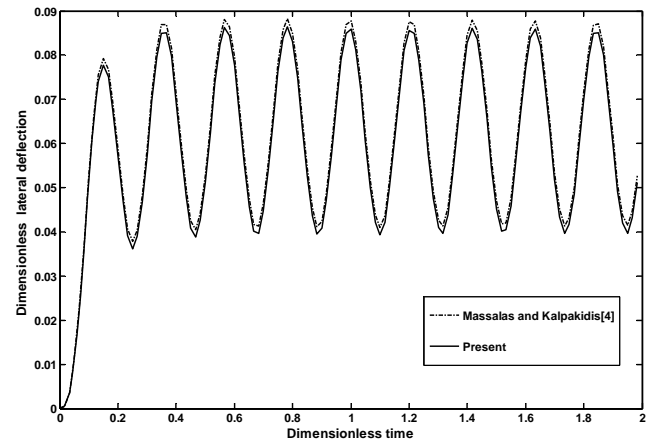


**Fig. 2:** Deflection history of an aluminum beam at midpoint with the coupled thermoelasticity assumption.

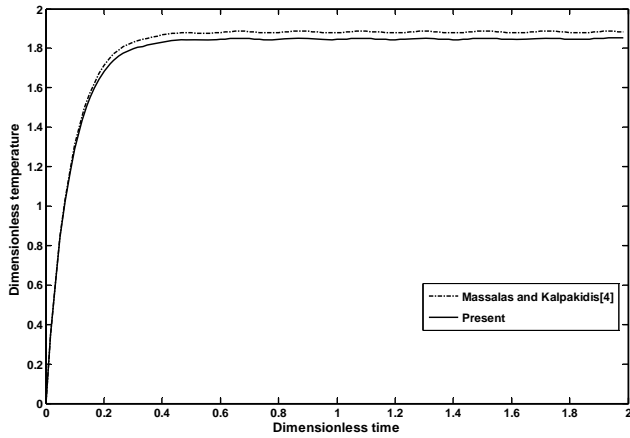


**Fig. 3:** Temperature change history between upper and lower surfaces of an aluminum beam at midpoint with the coupled thermoelasticity assumption.

subjected to a step function thermal shock with the strength  $q=10^8$  W/m<sup>2</sup> while the lower side is subjected to convection to the surrounding ambient with coefficient of  $h_c = 10000$  W/m<sup>2</sup>°K.

**Tab.1:** Material properties of metal and ceramic constituents

Metal: $Ti - 6Al - 4V$	Ceramic: $ZrO_2$
$E_m = 66.2$ (Gpa)	$E_c = 117.0$ (Gpa)
$\nu = 0.322$	$\nu = 0.322$
$\alpha_m = 10.3 \times 10^{-6}$ (1/°K)	$\alpha_c = 7.11 \times 10^{-6}$ (1/°K)
$\rho_m = 4.41 \times 10^3$ (kg/m <sup>3</sup> )	$\rho_c = 5.6 \times 10^3$ (kg/m <sup>3</sup> )
$k_m = 18.1$ (W/mK)	$k_c = 2.036$ (W/mK)
$c_m = 808.3$ (J/kg K)	$c_c = 615.6$ (J/kg K)

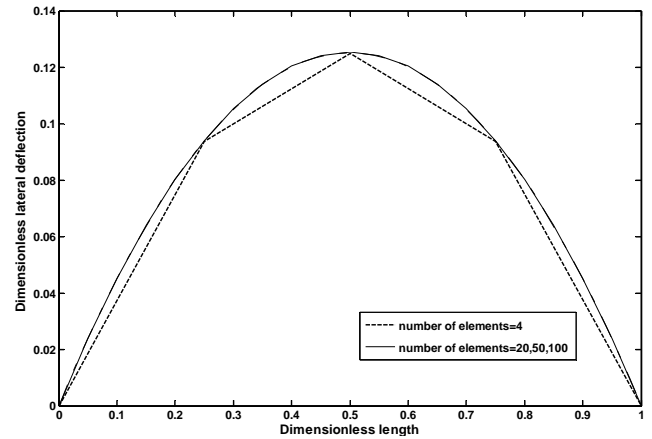
To check the rate of convergence of the Galerkin finite element method in relation to total number of the elements in the solution domain, fig. 4 is plotted for lateral deflection versus the length of the beam. The results are shown for 4, 20, 50, and 100 elements for full ceramic beam, where  $n=0$ , and for time  $\bar{t} = 3$ . It is seen that the results rapidly converge for 20 elements and higher. This rapid convergence is the advantage of  $C^1$ -continuous shape function and the Galerkin finite element method.

Figures 5 through 11 are presented to show the effect of the power law index of the functionally graded beam. The results in these figures are shown for the uncoupled thermoelasticity case. Figures 12 through 14 are discussed for the coupled case.

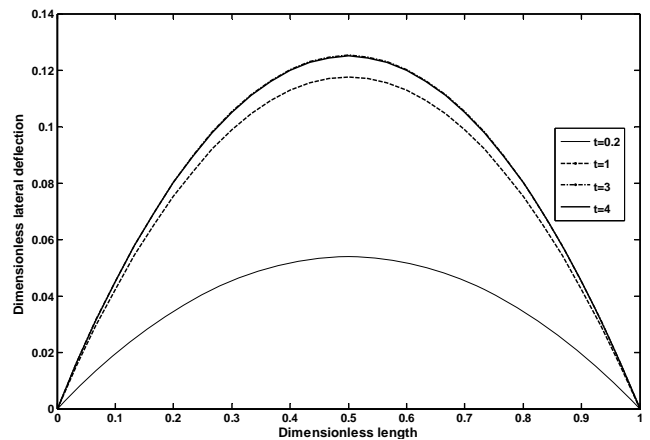
The distribution of lateral deflection along the length of a full ceramic beam is shown in fig. 5 for several times. The temperature distribution of the upper surface of the full ceramic beam is shown in fig. 6 for several times. As seen, the mechanical and thermal boundary conditions are satisfied during different times at the ends of the beam respectively in fig. 5 and fig. 6.

Figure 7 shows the lateral deflection of the middle length

of the beam with respect to time for different values of the power law index  $n$ . The curve associated with  $n=0$  corresponds



**Fig. 4:** Lateral deflection versus length for  $n=0$  (full ceramic) and  $\bar{t} = 3$ .



**Fig. 5:** Lateral deflection versus length for  $n=0$  (full ceramic) at different times.

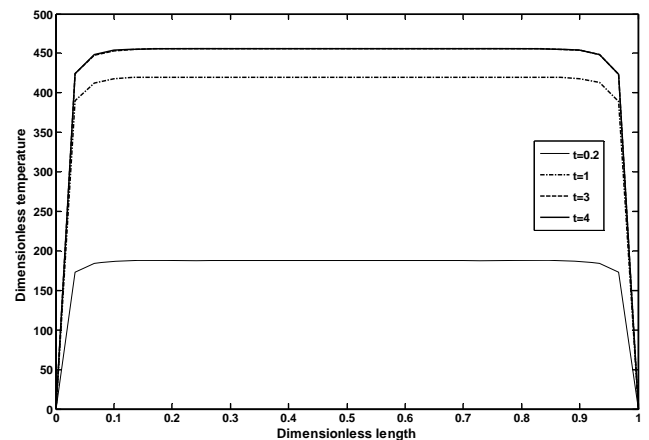


**Fig. 6:** Temperature distribution versus length at the upper surface of the full ceramic beam ( $n=0$ ).

to pure ceramic beam. The maximum lateral deflection, the frequency and the amplitude of the FGM beam vibration due to the thermal shock are dependent upon the mechanical and thermal properties of the beam. Therefore, when the power law index is changed, the FGM beam shows different behaviors. It is seen in fig. 7, with the increase of power law index  $n$ , the midpoint lateral deflection of the FGM beam is generally decreased because of decline in the temperature gradient in the beam. However, this condition does not always continue. As shown in fig. 8, when power law index  $n$  increases ( $n > 1$ ), the lateral deflection will be almost constant and minimum. Ceramic has greater modulus of elasticity rather than metal, while on the contrary the coefficient of thermal expansion of ceramic is smaller than metal one. This conflict causes noncontinuous behavior in the maximum lateral deflection for FGM beams subjected to the thermal shock. Further, for greater power law indices which provide most metal rich FGM, the lateral deflection and oscillation frequency begin slightly to increase. In general, the amplitude and frequency of the FGM beam vibration due to the applied thermal shock are increased when the beam constituent materials change from the ceramic-rich to the metal-rich.

Figure 9 shows the temperature history at the upper side and at midlength of the beam. Due to the applied step function thermal shock, the beam temperature peaks to a maximum value, and then diffuses along the time. The figure shows that for most metal rich FGM beam, (higher values of  $n$ ), the temperature distribution decreases in value due to higher thermal conductivity of metal. Figure 10 shows the distribution of temperature changes across the thickness direction at the midpoint of the beam at  $\bar{t} = 3$ . It can be concluded that for higher  $n$ , temperature distribution is changed slightly across the thickness of the FGM beam. By increasing in ceramic share of the beam, the gradient of temperature increases in value due to lower thermal conductivity of ceramic. That's why FGMs are used as thermal shields

Figure 11 shows lateral deflection history at the midpoint of an FGM beam ( $n=20$ ). The real solution is not usually distinguishable with the uncoupled for different materials. The damping effect of coupling factors is appeared by magnifying these factors 50 times. The coupled solution shows that coupling between strain and temperature field decreases the amplitude of the deflection's vibration due to the damping effect of coupling factor; furthermore, it deteriorates with respect to time, too. It is also observed that the frequency of the vibration for the coupled case increase with increasing time and also it is greater than the uncoupled case. When the temperature history on the upper side of the FGM beam ( $n=20$ ) is investigated for both coupled and uncoupled solution, no distinguishable difference is seen. This can be seen in the fig. 12. However, if the fig. 13 is zoomed it is seen that the coupled solution is vibrating around the uncoupled solution with very small amplitude because of the mathematical relation between the lateral deflection and the temperature.

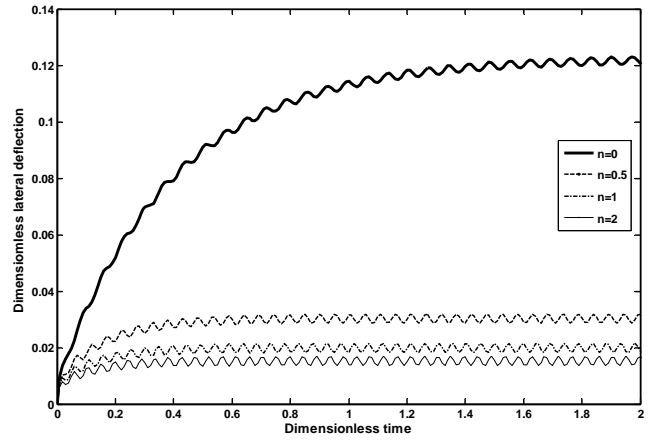


Fig. 7: Lateral deflection history at the midpoint of the beam for different power law indices.

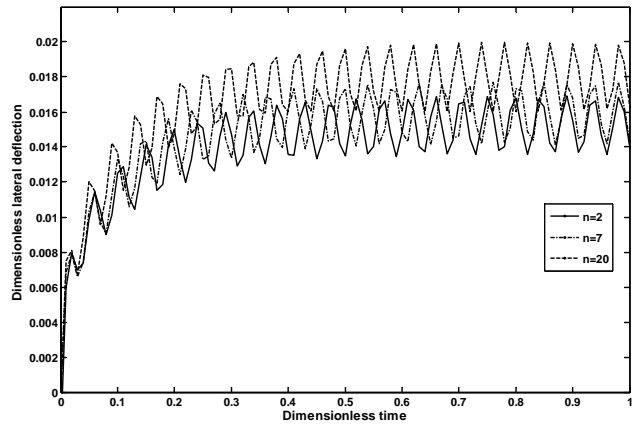


Fig. 8: Lateral deflection history at the midpoint of the beam for different power law indices.

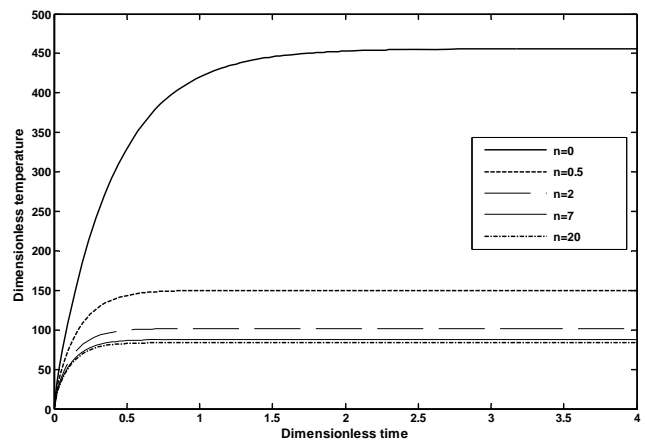
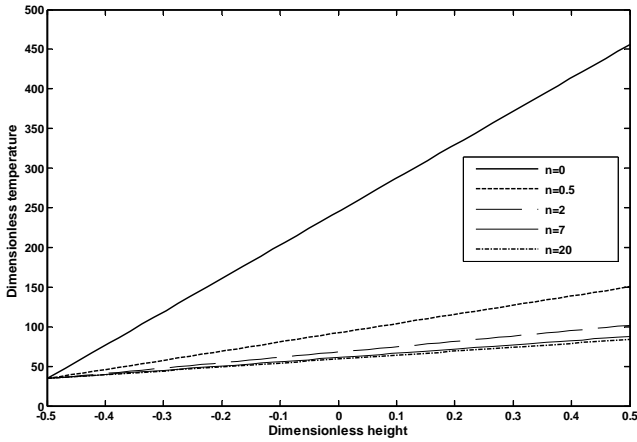
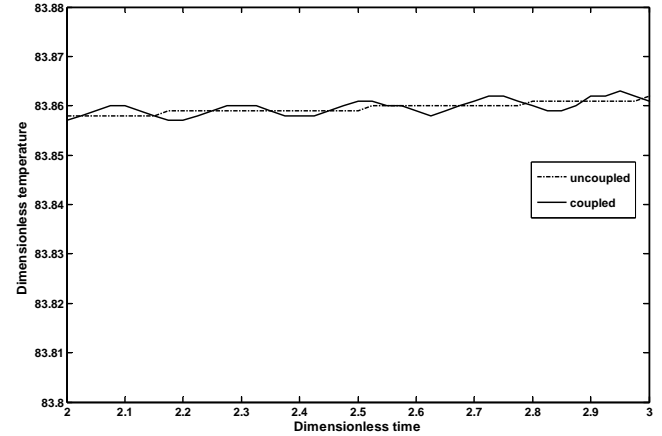


Fig. 9: Temperature change history at the midpoint of the beam at the upper side for different power law indices.



**Fig. 10:** Temperature change distribution at the midpoint of the beam across the thickness direction at  $\bar{t} = 3$  for different power law indices.



**Fig. 13:** Temperature change history at the midpoint of the FGM beam at the upper side for  $n=20$ , the coupling effects.

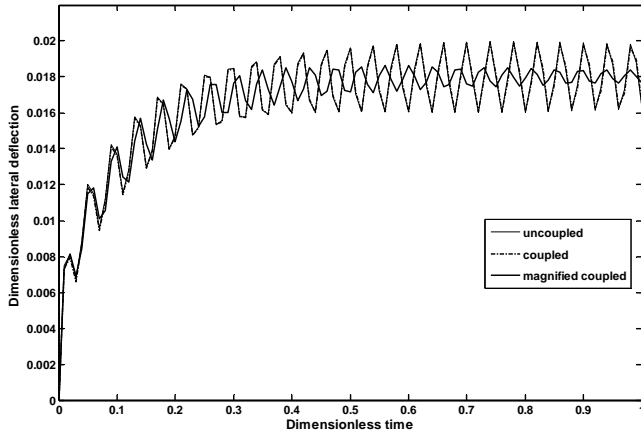


**Fig. 11:** Lateral deflection history at the midpoint of the FGM beam for  $n=20$ , the coupling effect.

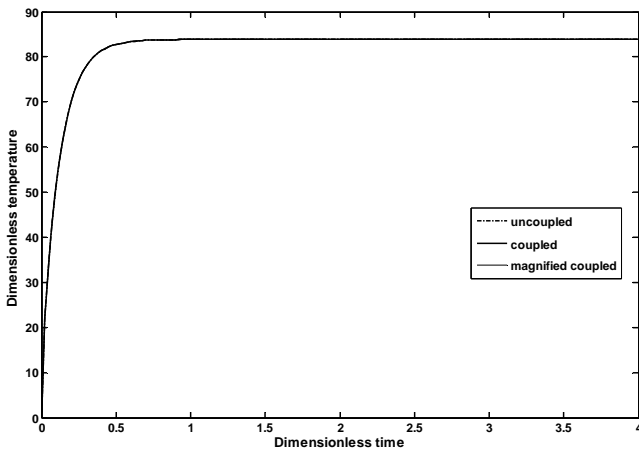


**Fig. 12:** Temperature change history at the midpoint of the FGM beam at the upper side for  $n=20$ , the coupling effects.

## CONCLUSIONS

In the present paper, the coupled thermoelasticity of a Timoshenko beam made of functionally graded material is investigated. The beam is subjected to a thermal shock of step function type on the upper side. The lower side of the beam is assumed to have convection to the surrounding ambient. Boundary conditions of the beam are taken to be simply supported and have ambient temperature at the ends of the beam. To solve the problem, the finite element Galerkin method with  $C^1$ -continuous shape functions is used. Moreover, to treat the time dependency, the Laplace transform technique is applied. The inverse Laplace transform is carried out numerically.

Results show that for larger values of power law indices which provide most metal rich FGM, since the thermal and mechanical properties of the beam are changed, the lateral deflection of an FGM beam does not decrease constantly due to applied thermal shock. There is an optimum value for FGM parameter in which the beams lateral deflection is minimum. By increasing in metal share of an FGM beam, distribution of temperature changes slightly across the thickness of the beam. Moreover, generally it can be said that there is no significant difference between coupled and uncoupled solution. However, the effect of coupling is like damping. It decreases the amplitude of vibration and increase the frequency of the vibrations with increasing time.

## REFERENCES

- [1] Jones P. J., 1966, "Thermoelastic vibration of beams", *Journal of Acoustical Society of America*, **39**, pp. 542-548.
- [2] McQuillen, E.J., Brull, M.A., 1970, "Dynamic thermoelastic response of cylindrical shell", *Journal of Applied Mechanics*, **37**, pp. 661-670.

- [3] A. G. Seibert and J. S. Rice, 1973 “Coupled thermally induced vibrations of beams”, *AIAA Journal*, **11**, pp. 1033-1035.
- [4] Massalas C.V., Kalpakidis V.K., 1983, “Coupled thermoelastic vibration of a simply supported beam”, *Journal of Sound and Vibration*, **88**, pp. 425-429.
- [5] Massalas C.V., Kalpakidis V.K., 1984, “Coupled thermoelastic vibration of a Timoshenko beam”, *Letter of Applied Engineering Science* **22**, pp. 459-465.
- [6] Eslami M.R., Vahedi H., 1988, “Coupled thermoelasticity beam problems”, *AIAA Journal*, **63**, pp. 662-665.
- [7] Maruthi D.R., Sinha P.K., 1997, “Finite element coupled thermostructural analysis of composite beams”, *Computers and Structures*, **63**, pp. 539-549.
- [8] Eslami M. R., Shakeri M., Ohadi A. R., Shiari B., 1999, “Coupled thermoelasticity of shells of revolution effect of normal stress and coupling”, *AIAA Journal*. **37 (2)**, pp. 1–9.
- [9] Manoach E., Ribeiro P., 2004, “Coupled thermoelastic large amplitude vibrations of Timoshenko beams”, *Journal of Mechanical Science*, **46**, pp. 1589-1606.
- [10] Sankar B. V., 2001, “An elasticity solution for functionally graded beams”, *Journal of Composites Science and Technology*, **61**, pp. 686-696.
- [11] Sankar B. V., Tzeng T.J., 2002, “Thermal stresses in functionally graded beams”, *AIAA Journal*, **40**, pp.1228-1232.
- [12] Bahtui A. and Eslami M. R., 2007, “Coupled Thermoelasticity of Functionally Graded Cylindrical Shells”, *Mechanics Research Communication*, **37 (1)**, pp. 1-18.
- [13] Durbin, F., 1973, “Numerical inversion of Laplace transforms”, *Computational Journal*, **17 (4)**, pp. 371–376.